

Improved measurement of the semileptonic decay  $D_s^+ \rightarrow K^0 e^+ \nu_e$ 

M. Ablikim<sup>1</sup>, M. N. Achasov<sup>4,c</sup>, P. Adlarson<sup>76</sup>, O. Afedulidis<sup>3</sup>, X. C. Ai<sup>81</sup>, R. Aliberti<sup>35</sup>, A. Amoroso<sup>75A,75C</sup>, Q. An<sup>72,58,a</sup>, Y. Bai<sup>57</sup>, O. Bakina<sup>36</sup>, I. Balossino<sup>29A</sup>, Y. Ban<sup>46,h</sup>, H.-R. Bao<sup>64</sup>, V. Batozskaya<sup>1,44</sup>, K. Begzsuren<sup>32</sup>, N. Berger<sup>35</sup>, M. Berlowski<sup>44</sup>, M. Bertani<sup>28A</sup>, D. Bettoni<sup>29A</sup>, F. Bianchi<sup>75A,75C</sup>, E. Bianco<sup>75A,75C</sup>, A. Bortone<sup>75A,75C</sup>, I. Boyko<sup>36</sup>, R. A. Briere<sup>5</sup>, A. Brueggemann<sup>69</sup>, H. Cai<sup>77</sup>, X. Cai<sup>1,58</sup>, A. Calcaterra<sup>28A</sup>, G. F. Cao<sup>1,64</sup>, N. Cao<sup>1,64</sup>, S. A. Cetin<sup>62A</sup>, J. F. Chang<sup>1,58</sup>, G. R. Che<sup>43</sup>, G. Chelkov<sup>36,b</sup>, C. Chen<sup>43</sup>, C. H. Chen<sup>9</sup>, Chao Chen<sup>55</sup>, G. Chen<sup>1</sup>, H. S. Chen<sup>1,64</sup>, H. Y. Chen<sup>20</sup>, M. L. Chen<sup>1,58,64</sup>, S. J. Chen<sup>42</sup>, S. L. Chen<sup>45</sup>, S. M. Chen<sup>61</sup>, T. Chen<sup>1,64</sup>, X. R. Chen<sup>31,64</sup>, X. T. Chen<sup>1,64</sup>, Y. B. Chen<sup>1,58</sup>, Y. Q. Chen<sup>34</sup>, Z. J. Chen<sup>25,i</sup>, Z. Y. Chen<sup>1,64</sup>, S. K. Choi<sup>10</sup>, G. Cibinetto<sup>29A</sup>, F. Cossio<sup>75C</sup>, J. J. Cui<sup>50</sup>, H. L. Dai<sup>1,58</sup>, J. P. Dai<sup>79</sup>, A. Dbeyssi<sup>18</sup>, R. E. de Boer<sup>3</sup>, D. Dedovich<sup>36</sup>, C. Q. Deng<sup>73</sup>, Z. Y. Deng<sup>1</sup>, A. Denig<sup>35</sup>, I. Denysenko<sup>36</sup>, M. Destefanis<sup>75A,75C</sup>, F. De Mori<sup>75A,75C</sup>, B. Ding<sup>67,1</sup>, X. X. Ding<sup>46,h</sup>, Y. Ding<sup>34</sup>, Y. Ding<sup>40</sup>, J. Dong<sup>1,58</sup>, L. Y. Dong<sup>1,64</sup>, M. Y. Dong<sup>1,58,64</sup>, X. Dong<sup>77</sup>, M. C. Du<sup>1</sup>, S. X. Du<sup>81</sup>, Y. Y. Duan<sup>55</sup>, Z. H. Duan<sup>42</sup>, P. Egorov<sup>36,b</sup>, Y. H. Fan<sup>45</sup>, J. Fang<sup>59</sup>, J. Fang<sup>1,58</sup>, S. S. Fang<sup>1,64</sup>, W. X. Fang<sup>1</sup>, Y. Fang<sup>1</sup>, Y. Q. Fang<sup>1,58</sup>, R. Farinelli<sup>29A</sup>, L. Fava<sup>75B,75C</sup>, F. Feldbauer<sup>3</sup>, G. Felici<sup>28A</sup>, C. Q. Feng<sup>72,58</sup>, J. H. Feng<sup>59</sup>, Y. T. Feng<sup>72,58</sup>, M. Fritsch<sup>3</sup>, C. D. Fu<sup>1</sup>, J. L. Fu<sup>64</sup>, Y. W. Fu<sup>1,64</sup>, H. Gao<sup>64</sup>, X. B. Gao<sup>41</sup>, Y. N. Gao<sup>46,h</sup>, Yang Gao<sup>72,58</sup>, S. Garbolino<sup>75C</sup>, I. Garzia<sup>29A,29B</sup>, L. Ge<sup>81</sup>, P. T. Ge<sup>19</sup>, Z. W. Ge<sup>42</sup>, C. Geng<sup>59</sup>, E. M. Gersabeck<sup>68</sup>, A. Gilman<sup>70</sup>, K. Goetzen<sup>13</sup>, L. Gong<sup>40</sup>, W. X. Gong<sup>1,58</sup>, W. Gradl<sup>35</sup>, S. Gramigna<sup>29A,29B</sup>, M. Greco<sup>75A,75C</sup>, M. H. Gu<sup>1,58</sup>, Y. T. Gu<sup>15</sup>, C. Y. Guan<sup>1,64</sup>, A. Q. Guo<sup>31,64</sup>, L. B. Guo<sup>41</sup>, M. J. Guo<sup>50</sup>, R. P. Guo<sup>49</sup>, Y. P. Guo<sup>12,g</sup>, A. Guskov<sup>36,b</sup>, J. Gutierrez<sup>27</sup>, K. L. Han<sup>64</sup>, T. T. Han<sup>1</sup>, F. Hanisch<sup>3</sup>, X. Q. Hao<sup>19</sup>, F. A. Harris<sup>66</sup>, K. K. He<sup>55</sup>, K. L. He<sup>1,64</sup>, F. H. Heinsius<sup>3</sup>, C. H. Heinz<sup>35</sup>, Y. K. Heng<sup>1,58,64</sup>, C. Herold<sup>60</sup>, T. Holtmann<sup>3</sup>, P. C. Hong<sup>34</sup>, G. Y. Hou<sup>1,64</sup>, X. T. Hou<sup>1,64</sup>, Y. R. Hou<sup>64</sup>, Z. L. Hou<sup>1</sup>, B. Y. Hu<sup>59</sup>, H. M. Hu<sup>1,64</sup>, J. F. Hu<sup>56,j</sup>, S. L. Hu<sup>12,g</sup>, T. Hu<sup>1,58,64</sup>, Y. Hu<sup>1</sup>, G. S. Huang<sup>72,58</sup>, K. X. Huang<sup>59</sup>, L. Q. Huang<sup>31,64</sup>, X. T. Huang<sup>50</sup>, Y. P. Huang<sup>1</sup>, Y. S. Huang<sup>59</sup>, T. Hussain<sup>74</sup>, F. Hölzken<sup>3</sup>, N. Hüsken<sup>35</sup>, N. in der Wiesche<sup>69</sup>, J. Jackson<sup>27</sup>, S. Janchiv<sup>32</sup>, J. H. Jeong<sup>10</sup>, Q. Ji<sup>1</sup>, Q. P. Ji<sup>19</sup>, W. Ji<sup>1,64</sup>, X. B. Ji<sup>1,64</sup>, X. L. Ji<sup>1,58</sup>, Y. Y. Ji<sup>50</sup>, X. Q. Jia<sup>50</sup>, Z. K. Jia<sup>72,58</sup>, D. Jiang<sup>1,64</sup>, H. B. Jiang<sup>77</sup>, P. C. Jiang<sup>46,h</sup>, S. S. Jiang<sup>39</sup>, T. J. Jiang<sup>16</sup>, X. S. Jiang<sup>1,58,64</sup>, Y. Jiang<sup>64</sup>, J. B. Jiao<sup>50</sup>, J. K. Jiao<sup>34</sup>, Z. Jiao<sup>23</sup>, S. Jin<sup>42</sup>, Y. Jin<sup>67</sup>, M. Q. Jing<sup>1,64</sup>, X. M. Jing<sup>64</sup>, T. Johansson<sup>76</sup>, S. Kabana<sup>33</sup>, N. Kalantar-Nayestanaki<sup>65</sup>, X. L. Kang<sup>9</sup>, X. S. Kang<sup>40</sup>, M. Kavatsyuk<sup>65</sup>, B. C. Ke<sup>81</sup>, V. Khachatryan<sup>27</sup>, A. Khoukaz<sup>69</sup>, R. Kiuchi<sup>1</sup>, O. B. Kolcu<sup>62A</sup>, B. Kopf<sup>3</sup>, M. Kuessner<sup>3</sup>, X. Kui<sup>1,64</sup>, N. Kumar<sup>26</sup>, A. Kupsc<sup>44,76</sup>, W. Kühn<sup>37</sup>, J. J. Lane<sup>68</sup>, L. Lavezzi<sup>75A,75C</sup>, T. T. Lei<sup>72,58</sup>, Z. H. Lei<sup>72,58</sup>, M. Lellmann<sup>35</sup>, T. Lenz<sup>35</sup>, C. Li<sup>47</sup>, C. Li<sup>43</sup>, C. H. Li<sup>39</sup>, Cheng Li<sup>72,58</sup>, D. M. Li<sup>81</sup>, F. Li<sup>1,58</sup>, G. Li<sup>1</sup>, H. B. Li<sup>1,64</sup>, H. J. Li<sup>19</sup>, H. N. Li<sup>56,j</sup>, Hui Li<sup>43</sup>, J. R. Li<sup>61</sup>, J. S. Li<sup>59</sup>, K. Li<sup>1</sup>, L. J. Li<sup>1,64</sup>, L. K. Li<sup>1</sup>, Lei Li<sup>48</sup>, M. H. Li<sup>43</sup>, P. R. Li<sup>38,k,l</sup>, Q. M. Li<sup>1,64</sup>, Q. X. Li<sup>50</sup>, R. Li<sup>17,31</sup>, S. X. Li<sup>12</sup>, T. Li<sup>50</sup>, W. D. Li<sup>1,64</sup>, W. G. Li<sup>1,a</sup>, X. Li<sup>1,64</sup>, X. H. Li<sup>72,58</sup>, X. L. Li<sup>50</sup>, X. Y. Li<sup>1,64</sup>, X. Z. Li<sup>59</sup>, Y. G. Li<sup>46,h</sup>, Z. J. Li<sup>59</sup>, Z. Y. Li<sup>79</sup>, C. Liang<sup>42</sup>, H. Liang<sup>72,58</sup>, H. Liang<sup>1,64</sup>, Y. F. Liang<sup>54</sup>, Y. T. Liang<sup>31,64</sup>, G. R. Liao<sup>14</sup>, Y. P. Liao<sup>1,64</sup>, J. Libby<sup>26</sup>, A. Limphirat<sup>60</sup>, C. C. Lin<sup>55</sup>, D. X. Lin<sup>31,64</sup>, T. Lin<sup>1</sup>, B. J. Liu<sup>1</sup>, B. X. Liu<sup>77</sup>, C. Liu<sup>34</sup>, C. X. Liu<sup>1</sup>, F. Liu<sup>1</sup>, F. H. Liu<sup>53</sup>, Feng Liu<sup>6</sup>, G. M. Liu<sup>56,j</sup>, H. Liu<sup>38,k,l</sup>, H. B. Liu<sup>15</sup>, H. H. Liu<sup>1</sup>, H. M. Liu<sup>1,64</sup>, Huihui Liu<sup>21</sup>, J. B. Liu<sup>72,58</sup>, J. Y. Liu<sup>1,64</sup>, K. Liu<sup>38,k,l</sup>, K. Y. Liu<sup>40</sup>, Ke Liu<sup>22</sup>, L. Liu<sup>72,58</sup>, L. C. Liu<sup>43</sup>, Lu Liu<sup>43</sup>, M. H. Liu<sup>12,g</sup>, N. Liu<sup>47</sup>, P. L. Liu<sup>1</sup>, Q. Liu<sup>64</sup>, S. B. Liu<sup>72,58</sup>, T. Liu<sup>12,g</sup>, W. K. Liu<sup>43</sup>, W. M. Liu<sup>72,58</sup>, X. Liu<sup>38,k,l</sup>, X. Liu<sup>39</sup>, Y. Liu<sup>38,k,l</sup>, Y. Liu<sup>81</sup>, Y. B. Liu<sup>43</sup>, Z. A. Liu<sup>1,58,64</sup>, Z. D. Liu<sup>9</sup>, Z. Q. Liu<sup>50</sup>, X. C. Lou<sup>1,58,64</sup>, F. X. Lu<sup>59</sup>, H. J. Lu<sup>23</sup>, J. G. Lu<sup>1,58</sup>, X. L. Lu<sup>1</sup>, Y. Lu<sup>7</sup>, Y. P. Lu<sup>1,58</sup>, Z. H. Lu<sup>1,64</sup>, C. L. Luo<sup>41</sup>, J. R. Luo<sup>59</sup>, M. X. Luo<sup>80</sup>, T. Luo<sup>12,g</sup>, X. L. Luo<sup>1,58</sup>, X. R. Lyu<sup>64</sup>, Y. F. Lyu<sup>43</sup>, F. C. Ma<sup>40</sup>, H. Ma<sup>79</sup>, H. L. Ma<sup>1</sup>, J. L. Ma<sup>1,64</sup>, L. L. Ma<sup>50</sup>, L. R. Ma<sup>67</sup>, M. M. Ma<sup>1,64</sup>, Q. M. Ma<sup>1</sup>, R. Q. Ma<sup>1,64</sup>, T. Ma<sup>72,58</sup>, X. T. Ma<sup>1,64</sup>, X. Y. Ma<sup>1,58</sup>, Y. Ma<sup>46,h</sup>, Y. M. Ma<sup>31</sup>, F. E. Maas<sup>18</sup>, M. Maggiora<sup>75A,75C</sup>, S. Malde<sup>70</sup>, Y. J. Mao<sup>46,h</sup>, Z. P. Mao<sup>1</sup>, S. Marcello<sup>75A,75C</sup>, Z. X. Meng<sup>67</sup>, J. G. Messchendorp<sup>13,65</sup>, G. Mezzadri<sup>29A</sup>, H. Miao<sup>1,64</sup>, T. J. Min<sup>42</sup>, R. E. Mitchell<sup>27</sup>, X. H. Mo<sup>1,58,64</sup>, B. Moses<sup>27</sup>, N. Yu. Muchnoi<sup>4,c</sup>, J. Muskalla<sup>35</sup>, Y. Nefedov<sup>36</sup>, F. Nerling<sup>18,e</sup>, L. S. Nie<sup>20</sup>, I. B. Nikolaev<sup>4,c</sup>, Z. Ning<sup>1,58</sup>, S. Nisar<sup>11,m</sup>, Q. L. Niu<sup>38,k,l</sup>, W. D. Niu<sup>55</sup>, Y. Niu<sup>50</sup>, S. L. Olsen<sup>64</sup>, Q. Ouyang<sup>1,58,64</sup>, S. Pacetti<sup>28B,28C</sup>, X. Pan<sup>55</sup>, Y. Pan<sup>57</sup>, A. Pathak<sup>34</sup>, Y. P. Pei<sup>72,58</sup>, M. Pelizaeus<sup>3</sup>, H. P. Peng<sup>72,58</sup>, Y. Y. Peng<sup>38,k,l</sup>, K. Peters<sup>13,e</sup>, J. L. Ping<sup>41</sup>, R. G. Ping<sup>1,64</sup>, S. Plura<sup>35</sup>, V. Prasad<sup>33</sup>, F. Z. Qi<sup>1</sup>, H. Qi<sup>72,58</sup>, H. R. Qi<sup>61</sup>, M. Qi<sup>42</sup>, T. Y. Qi<sup>12,g</sup>, S. Qian<sup>1,58</sup>, W. B. Qian<sup>64</sup>, C. F. Qiao<sup>64</sup>, X. K. Qiao<sup>81</sup>, J. J. Qin<sup>73</sup>, L. Q. Qin<sup>14</sup>, L. Y. Qin<sup>72,58</sup>, X. P. Qin<sup>12,g</sup>, X. S. Qin<sup>50</sup>, Z. H. Qin<sup>1,58</sup>, J. F. Qiu<sup>1</sup>, Z. H. Qu<sup>73</sup>, C. F. Redmer<sup>35</sup>, K. J. Ren<sup>39</sup>, A. Rivetti<sup>75C</sup>, M. Rolo<sup>75C</sup>, G. Rong<sup>1,64</sup>, Ch. Rosner<sup>18</sup>, S. N. Ruan<sup>43</sup>, N. Salone<sup>44</sup>, A. Sarantsev<sup>36,d</sup>, Y. Schelhaas<sup>35</sup>, K. Schoenning<sup>76</sup>, M. Scodreggio<sup>29A</sup>, K. Y. Shan<sup>12,g</sup>, W. Shan<sup>24</sup>, X. Y. Shan<sup>72,58</sup>, Z. J. Shang<sup>38,k,l</sup>, J. F. Shangguan<sup>16</sup>, L. G. Shao<sup>1,64</sup>, M. Shao<sup>72,58</sup>, C. P. Shen<sup>12,g</sup>, H. F. Shen<sup>1,8</sup>, W. H. Shen<sup>64</sup>, X. Y. Shen<sup>1,64</sup>, B. A. Shi<sup>64</sup>, H. Shi<sup>72,58</sup>, H. C. Shi<sup>72,58</sup>, J. L. Shi<sup>12,g</sup>, J. Y. Shi<sup>1</sup>, Q. Q. Shi<sup>55</sup>, S. Y. Shi<sup>73</sup>, X. Shi<sup>1,58</sup>, J. J. Song<sup>19</sup>, T. Z. Song<sup>59</sup>, W. M. Song<sup>34,1</sup>, Y. J. Song<sup>12,g</sup>, Y. X. Song<sup>46,h,m</sup>, S. Sosio<sup>75A,75C</sup>, S. Spataro<sup>75A,75C</sup>, F. Stieler<sup>35</sup>, S. S. Su<sup>40</sup>,

Y. J. Su<sup>64</sup>, G. B. Sun<sup>77</sup>, G. X. Sun<sup>1</sup>, H. Sun<sup>64</sup>, H. K. Sun<sup>1</sup>, J. F. Sun<sup>19</sup>, K. Sun<sup>61</sup>, L. Sun<sup>77</sup>, S. S. Sun<sup>1,64</sup>, T. Sun<sup>51,f</sup>, W. Y. Sun<sup>34</sup>, Y. Sun<sup>9</sup>, Y. J. Sun<sup>72,58</sup>, Y. Z. Sun<sup>1</sup>, Z. Q. Sun<sup>1,64</sup>, Z. T. Sun<sup>50</sup>, C. J. Tang<sup>54</sup>, G. Y. Tang<sup>1</sup>, J. Tang<sup>59</sup>, M. Tang<sup>72,58</sup>, Y. A. Tang<sup>77</sup>, L. Y. Tao<sup>73</sup>, Q. T. Tao<sup>25,i</sup>, M. Tat<sup>70</sup>, J. X. Teng<sup>72,58</sup>, V. Thoren<sup>76</sup>, W. H. Tian<sup>59</sup>, Y. Tian<sup>31,64</sup>, Z. F. Tian<sup>77</sup>, I. Uman<sup>62B</sup>, Y. Wan<sup>55</sup>, S. J. Wang<sup>50</sup>, B. Wang<sup>1</sup>, B. L. Wang<sup>64</sup>, Bo Wang<sup>72,58</sup>, D. Y. Wang<sup>46,h</sup>, F. Wang<sup>73</sup>, H. J. Wang<sup>38,k,l</sup>, J. J. Wang<sup>77</sup>, J. P. Wang<sup>50</sup>, K. Wang<sup>1,58</sup>, L. L. Wang<sup>1</sup>, M. Wang<sup>50</sup>, N. Y. Wang<sup>64</sup>, S. Wang<sup>38,k,l</sup>, S. Wang<sup>12,g</sup>, T. Wang<sup>12,g</sup>, T. J. Wang<sup>43</sup>, W. Wang<sup>59</sup>, W. Wang<sup>73</sup>, W. P. Wang<sup>35,72,o</sup>, X. Wang<sup>46,h</sup>, X. F. Wang<sup>38,k,l</sup>, X. J. Wang<sup>39</sup>, X. L. Wang<sup>12,g</sup>, X. N. Wang<sup>1</sup>, Y. Wang<sup>61</sup>, Y. D. Wang<sup>45</sup>, Y. F. Wang<sup>1,58,64</sup>, Y. L. Wang<sup>19</sup>, Y. N. Wang<sup>45</sup>, Y. Q. Wang<sup>1</sup>, Yaqian Wang<sup>17</sup>, Yi Wang<sup>61</sup>, Z. Wang<sup>1,58</sup>, Z. L. Wang<sup>73</sup>, Z. Y. Wang<sup>1,64</sup>, Ziyi Wang<sup>64</sup>, D. H. Wei<sup>14</sup>, F. Weidner<sup>69</sup>, S. P. Wen<sup>1</sup>, Y. R. Wen<sup>39</sup>, U. Wiedner<sup>3</sup>, G. Wilkinson<sup>70</sup>, M. Wolke<sup>76</sup>, L. Wollenberg<sup>3</sup>, C. Wu<sup>39</sup>, J. F. Wu<sup>1,8</sup>, L. H. Wu<sup>1</sup>, L. J. Wu<sup>1,64</sup>, X. Wu<sup>12,g</sup>, X. H. Wu<sup>34</sup>, Y. Wu<sup>72,58</sup>, Y. H. Wu<sup>55</sup>, Y. J. Wu<sup>31</sup>, Z. Wu<sup>1,58</sup>, L. Xia<sup>72,58</sup>, X. M. Xian<sup>39</sup>, B. H. Xiang<sup>1,64</sup>, T. Xiang<sup>46,h</sup>, D. Xiao<sup>38,k,l</sup>, G. Y. Xiao<sup>42</sup>, S. Y. Xiao<sup>1</sup>, Y. L. Xiao<sup>12,g</sup>, Z. J. Xiao<sup>41</sup>, C. Xie<sup>42</sup>, X. H. Xie<sup>46,h</sup>, Y. Xie<sup>50</sup>, Y. G. Xie<sup>1,58</sup>, Y. H. Xie<sup>6</sup>, Z. P. Xie<sup>72,58</sup>, T. Y. Xing<sup>1,64</sup>, C. F. Xu<sup>1,64</sup>, C. J. Xu<sup>59</sup>, G. F. Xu<sup>1</sup>, H. Y. Xu<sup>67,2,p</sup>, M. Xu<sup>72,58</sup>, Q. J. Xu<sup>16</sup>, Q. N. Xu<sup>30</sup>, W. Xu<sup>1</sup>, W. L. Xu<sup>67</sup>, X. P. Xu<sup>55</sup>, Y. Xu<sup>40</sup>, Y. C. Xu<sup>78</sup>, Z. S. Xu<sup>64</sup>, F. Yan<sup>12,g</sup>, L. Yan<sup>12,g</sup>, W. B. Yan<sup>72,58</sup>, W. C. Yan<sup>81</sup>, X. Q. Yan<sup>1,64</sup>, H. J. Yang<sup>51,f</sup>, H. L. Yang<sup>34</sup>, H. X. Yang<sup>1</sup>, T. Yang<sup>1</sup>, Y. Yang<sup>12,g</sup>, Y. F. Yang<sup>1,64</sup>, Y. F. Yang<sup>43</sup>, Y. X. Yang<sup>1,64</sup>, Z. W. Yang<sup>38,k,l</sup>, Z. P. Yao<sup>50</sup>, M. Ye<sup>1,58</sup>, M. H. Ye<sup>8</sup>, J. H. Yin<sup>1</sup>, Junhao Yin<sup>43</sup>, Z. Y. You<sup>59</sup>, B. X. Yu<sup>1,58,64</sup>, C. X. Yu<sup>43</sup>, G. Yu<sup>1,64</sup>, J. S. Yu<sup>25,i</sup>, M. C. Yu<sup>40</sup>, T. Yu<sup>73</sup>, X. D. Yu<sup>46,h</sup>, Y. C. Yu<sup>81</sup>, C. Z. Yuan<sup>1,64</sup>, J. Yuan<sup>34</sup>, J. Yuan<sup>45</sup>, L. Yuan<sup>2</sup>, S. C. Yuan<sup>1,64</sup>, Y. Yuan<sup>1,64</sup>, Z. Y. Yuan<sup>59</sup>, C. X. Yue<sup>39</sup>, A. A. Zafar<sup>74</sup>, F. R. Zeng<sup>50</sup>, S. H. Zeng<sup>63A,63B,63C,63D</sup>, X. Zeng<sup>12,g</sup>, Y. Zeng<sup>25,i</sup>, Y. J. Zeng<sup>1,64</sup>, Y. J. Zeng<sup>59</sup>, X. Y. Zhai<sup>34</sup>, Y. C. Zhai<sup>50</sup>, Y. H. Zhan<sup>59</sup>, A. Q. Zhang<sup>1,64</sup>, B. L. Zhang<sup>1,64</sup>, B. X. Zhang<sup>1</sup>, D. H. Zhang<sup>43</sup>, G. Y. Zhang<sup>19</sup>, H. Zhang<sup>81</sup>, H. Zhang<sup>72,58</sup>, H. C. Zhang<sup>1,58,64</sup>, H. H. Zhang<sup>34</sup>, H. H. Zhang<sup>59</sup>, H. Q. Zhang<sup>1,58,64</sup>, H. R. Zhang<sup>72,58</sup>, H. Y. Zhang<sup>1,58</sup>, J. Zhang<sup>81</sup>, J. Zhang<sup>59</sup>, J. J. Zhang<sup>52</sup>, J. L. Zhang<sup>20</sup>, J. Q. Zhang<sup>41</sup>, J. S. Zhang<sup>12,g</sup>, J. W. Zhang<sup>1,58,64</sup>, J. X. Zhang<sup>38,k,l</sup>, J. Y. Zhang<sup>1</sup>, J. Z. Zhang<sup>1,64</sup>, Jianyu Zhang<sup>64</sup>, L. M. Zhang<sup>61</sup>, Lei Zhang<sup>42</sup>, P. Zhang<sup>1,64</sup>, Q. Y. Zhang<sup>34</sup>, R. Y. Zhang<sup>38,k,l</sup>, S. H. Zhang<sup>1,64</sup>, Shulei Zhang<sup>25,i</sup>, X. D. Zhang<sup>45</sup>, X. M. Zhang<sup>1</sup>, X. Y. Zhang<sup>40</sup>, X. Y. Zhang<sup>50</sup>, Y. Zhang<sup>73</sup>, Y. Zhang<sup>1</sup>, Y. T. Zhang<sup>81</sup>, Y. H. Zhang<sup>1,58</sup>, Y. M. Zhang<sup>39</sup>, Yan Zhang<sup>72,58</sup>, Z. D. Zhang<sup>1</sup>, Z. H. Zhang<sup>1</sup>, Z. L. Zhang<sup>34</sup>, Z. Y. Zhang<sup>43</sup>, Z. Y. Zhang<sup>77</sup>, Z. Z. Zhang<sup>45</sup>, G. Zhao<sup>1</sup>, J. Y. Zhao<sup>1,64</sup>, J. Z. Zhao<sup>1,58</sup>, L. Zhao<sup>1</sup>, Lei Zhao<sup>72,58</sup>, M. G. Zhao<sup>43</sup>, N. Zhao<sup>79</sup>, R. P. Zhao<sup>64</sup>, S. J. Zhao<sup>81</sup>, Y. B. Zhao<sup>1,58</sup>, Y. X. Zhao<sup>31,64</sup>, Z. G. Zhao<sup>72,58</sup>, A. Zhemchugov<sup>36,b</sup>, B. Zheng<sup>73</sup>, B. M. Zheng<sup>34</sup>, J. P. Zheng<sup>1,58</sup>, W. J. Zheng<sup>1,64</sup>, Y. H. Zheng<sup>64</sup>, B. Zhong<sup>41</sup>, X. Zhong<sup>59</sup>, H. Zhou<sup>50</sup>, J. Y. Zhou<sup>34</sup>, L. P. Zhou<sup>1,64</sup>, S. Zhou<sup>6</sup>, X. Zhou<sup>77</sup>, X. K. Zhou<sup>6</sup>, X. R. Zhou<sup>72,58</sup>, X. Y. Zhou<sup>39</sup>, Y. Z. Zhou<sup>12,g</sup>, Z. C. Zhou<sup>20</sup>, A. N. Zhu<sup>64</sup>, J. Zhu<sup>43</sup>, K. Zhu<sup>1</sup>, K. J. Zhu<sup>1,58,64</sup>, K. S. Zhu<sup>12,g</sup>, L. Zhu<sup>34</sup>, L. X. Zhu<sup>64</sup>, S. H. Zhu<sup>71</sup>, T. J. Zhu<sup>12,g</sup>, W. D. Zhu<sup>41</sup>, Y. C. Zhu<sup>72,58</sup>, Z. A. Zhu<sup>1,64</sup>, J. H. Zou<sup>1</sup>, J. Zu<sup>72,58</sup>

(BESIII Collaboration)

<sup>1</sup> *Institute of High Energy Physics, Beijing 100049, People's Republic of China*

<sup>2</sup> *Beihang University, Beijing 100191, People's Republic of China*

<sup>3</sup> *Bochum Ruhr-University, D-44780 Bochum, Germany*

<sup>4</sup> *Budker Institute of Nuclear Physics SB RAS (BINP), Novosibirsk 630090, Russia*

<sup>5</sup> *Carnegie Mellon University, Pittsburgh, Pennsylvania 15213, USA*

<sup>6</sup> *Central China Normal University, Wuhan 430079, People's Republic of China*

<sup>7</sup> *Central South University, Changsha 410083, People's Republic of China*

<sup>8</sup> *China Center of Advanced Science and Technology, Beijing 100190, People's Republic of China*

<sup>9</sup> *China University of Geosciences, Wuhan 430074, People's Republic of China*

<sup>10</sup> *Chung-Ang University, Seoul, 06974, Republic of Korea*

<sup>11</sup> *COMSATS University Islamabad, Lahore Campus, Defence Road, Off Raiwind Road, 54000 Lahore, Pakistan*

<sup>12</sup> *Fudan University, Shanghai 200433, People's Republic of China*

<sup>13</sup> *GSI Helmholtzcentre for Heavy Ion Research GmbH, D-64291 Darmstadt, Germany*

<sup>14</sup> *Guangxi Normal University, Guilin 541004, People's Republic of China*

<sup>15</sup> *Guangxi University, Nanning 530004, People's Republic of China*

<sup>16</sup> *Hangzhou Normal University, Hangzhou 310036, People's Republic of China*

<sup>17</sup> *Hebei University, Baoding 071002, People's Republic of China*

<sup>18</sup> *Helmholtz Institute Mainz, Staudinger Weg 18, D-55099 Mainz, Germany*

<sup>19</sup> *Henan Normal University, Xinxiang 453007, People's Republic of China*

<sup>20</sup> *Henan University, Kaifeng 475004, People's Republic of China*

- <sup>21</sup> Henan University of Science and Technology, Luoyang 471003, People's Republic of China
- <sup>22</sup> Henan University of Technology, Zhengzhou 450001, People's Republic of China
- <sup>23</sup> Huangshan College, Huangshan 245000, People's Republic of China
- <sup>24</sup> Hunan Normal University, Changsha 410081, People's Republic of China
- <sup>25</sup> Hunan University, Changsha 410082, People's Republic of China
- <sup>26</sup> Indian Institute of Technology Madras, Chennai 600036, India
- <sup>27</sup> Indiana University, Bloomington, Indiana 47405, USA
- <sup>28</sup> INFN Laboratori Nazionali di Frascati, (A)INFN Laboratori Nazionali di Frascati, I-00044, Frascati, Italy; (B)INFN Sezione di Perugia, I-06100, Perugia, Italy; (C)University of Perugia, I-06100, Perugia, Italy
- <sup>29</sup> INFN Sezione di Ferrara, (A)INFN Sezione di Ferrara, I-44122, Ferrara, Italy; (B)University of Ferrara, I-44122, Ferrara, Italy
- <sup>30</sup> Inner Mongolia University, Hohhot 010021, People's Republic of China
- <sup>31</sup> Institute of Modern Physics, Lanzhou 730000, People's Republic of China
- <sup>32</sup> Institute of Physics and Technology, Peace Avenue 54B, Ulaanbaatar 13330, Mongolia
- <sup>33</sup> Instituto de Alta Investigación, Universidad de Tarapacá, Casilla 7D, Arica 1000000, Chile
- <sup>34</sup> Jilin University, Changchun 130012, People's Republic of China
- <sup>35</sup> Johannes Gutenberg University of Mainz, Johann-Joachim-Becher-Weg 45, D-55099 Mainz, Germany
- <sup>36</sup> Joint Institute for Nuclear Research, 141980 Dubna, Moscow region, Russia
- <sup>37</sup> Justus-Liebig-Universität Giessen, II. Physikalisches Institut, Heinrich-Buff-Ring 16, D-35392 Giessen, Germany
- <sup>38</sup> Lanzhou University, Lanzhou 730000, People's Republic of China
- <sup>39</sup> Liaoning Normal University, Dalian 116029, People's Republic of China
- <sup>40</sup> Liaoning University, Shenyang 110036, People's Republic of China
- <sup>41</sup> Nanjing Normal University, Nanjing 210023, People's Republic of China
- <sup>42</sup> Nanjing University, Nanjing 210093, People's Republic of China
- <sup>43</sup> Nankai University, Tianjin 300071, People's Republic of China
- <sup>44</sup> National Centre for Nuclear Research, Warsaw 02-093, Poland
- <sup>45</sup> North China Electric Power University, Beijing 102206, People's Republic of China
- <sup>46</sup> Peking University, Beijing 100871, People's Republic of China
- <sup>47</sup> Qufu Normal University, Qufu 273165, People's Republic of China
- <sup>48</sup> Renmin University of China, Beijing 100872, People's Republic of China
- <sup>49</sup> Shandong Normal University, Jinan 250014, People's Republic of China
- <sup>50</sup> Shandong University, Jinan 250100, People's Republic of China
- <sup>51</sup> Shanghai Jiao Tong University, Shanghai 200240, People's Republic of China
- <sup>52</sup> Shanxi Normal University, Linfen 041004, People's Republic of China
- <sup>53</sup> Shanxi University, Taiyuan 030006, People's Republic of China
- <sup>54</sup> Sichuan University, Chengdu 610064, People's Republic of China
- <sup>55</sup> Soochow University, Suzhou 215006, People's Republic of China
- <sup>56</sup> South China Normal University, Guangzhou 510006, People's Republic of China
- <sup>57</sup> Southeast University, Nanjing 211100, People's Republic of China
- <sup>58</sup> State Key Laboratory of Particle Detection and Electronics, Beijing 100049, Hefei 230026, People's Republic of China
- <sup>59</sup> Sun Yat-Sen University, Guangzhou 510275, People's Republic of China
- <sup>60</sup> Suranaree University of Technology, University Avenue 111, Nakhon Ratchasima 30000, Thailand
- <sup>61</sup> Tsinghua University, Beijing 100084, People's Republic of China
- <sup>62</sup> Turkish Accelerator Center Particle Factory Group, (A)Istinye University, 34010, Istanbul, Turkey; (B)Near East University, Nicosia, North Cyprus, 99138, Mersin 10, Turkey
- <sup>63</sup> University of Bristol, (A)H H Wills Physics Laboratory; (B)Tyndall Avenue; (C)Bristol; (D)BS8 1TL
- <sup>64</sup> University of Chinese Academy of Sciences, Beijing 100049, People's Republic of China
- <sup>65</sup> University of Groningen, NL-9747 AA Groningen, The Netherlands
- <sup>66</sup> University of Hawaii, Honolulu, Hawaii 96822, USA
- <sup>67</sup> University of Jinan, Jinan 250022, People's Republic of China
- <sup>68</sup> University of Manchester, Oxford Road, Manchester, M13 9PL, United Kingdom
- <sup>69</sup> University of Muenster, Wilhelm-Klemm-Strasse 9, 48149 Muenster, Germany

<sup>70</sup> *University of Oxford, Keble Road, Oxford OX13RH, United Kingdom*

<sup>71</sup> *University of Science and Technology Liaoning, Anshan 114051, People's Republic of China*

<sup>72</sup> *University of Science and Technology of China, Hefei 230026, People's Republic of China*

<sup>73</sup> *University of South China, Hengyang 421001, People's Republic of China*

<sup>74</sup> *University of the Punjab, Lahore-54590, Pakistan*

<sup>75</sup> *University of Turin and INFN, (A)University of Turin, I-10125, Turin, Italy; (B)University of Eastern Piedmont, I-15121, Alessandria, Italy; (C)INFN, I-10125, Turin, Italy*

<sup>76</sup> *Uppsala University, Box 516, SE-75120 Uppsala, Sweden*

<sup>77</sup> *Wuhan University, Wuhan 430072, People's Republic of China*

<sup>78</sup> *Yantai University, Yantai 264005, People's Republic of China*

<sup>79</sup> *Yunnan University, Kunming 650500, People's Republic of China*

<sup>80</sup> *Zhejiang University, Hangzhou 310027, People's Republic of China*

<sup>81</sup> *Zhengzhou University, Zhengzhou 450001, People's Republic of China*

<sup>a</sup> *Deceased*

<sup>b</sup> *Also at the Moscow Institute of Physics and Technology, Moscow 141700, Russia*

<sup>c</sup> *Also at the Novosibirsk State University, Novosibirsk, 630090, Russia*

<sup>d</sup> *Also at the NRC "Kurchatov Institute", PNPI, 188300, Gatchina, Russia*

<sup>e</sup> *Also at Goethe University Frankfurt, 60323 Frankfurt am Main, Germany*

<sup>f</sup> *Also at Key Laboratory for Particle Physics, Astrophysics and Cosmology, Ministry of Education; Shanghai Key Laboratory for Particle Physics and Cosmology; Institute of Nuclear and Particle Physics, Shanghai 200240, People's Republic of China*

<sup>g</sup> *Also at Key Laboratory of Nuclear Physics and Ion-beam Application (MOE) and Institute of Modern Physics, Fudan University, Shanghai 200443, People's Republic of China*

<sup>h</sup> *Also at State Key Laboratory of Nuclear Physics and Technology, Peking University, Beijing 100871, People's Republic of China*

<sup>i</sup> *Also at School of Physics and Electronics, Hunan University, Changsha 410082, China*

<sup>j</sup> *Also at Guangdong Provincial Key Laboratory of Nuclear Science, Institute of Quantum Matter, South China Normal University, Guangzhou 510006, China*

<sup>k</sup> *Also at MOE Frontiers Science Center for Rare Isotopes, Lanzhou University, Lanzhou 730000, People's Republic of China*

<sup>l</sup> *Also at Lanzhou Center for Theoretical Physics, Lanzhou University, Lanzhou 730000, People's Republic of China*

<sup>m</sup> *Also at the Department of Mathematical Sciences, IBA, Karachi 75270, Pakistan*

<sup>n</sup> *Also at Ecole Polytechnique Federale de Lausanne (EPFL), CH-1015 Lausanne, Switzerland*

<sup>o</sup> *Also at Helmholtz Institute Mainz, Staudinger Weg 18, D-55099 Mainz, Germany*

<sup>p</sup> *Also at School of Physics, Beihang University, Beijing 100191, China*

Analyzing  $e^+e^-$  collision data corresponding to an integrated luminosity of  $7.33 \text{ fb}^{-1}$  collected at center-of-mass energies between 4.128 and 4.226 GeV with the BESIII detector, we measure the branching fraction of the semileptonic decay  $D_s^+ \rightarrow K^0 e^+ \nu_e$  to be  $(2.98 \pm 0.23 \pm 0.12) \times 10^{-3}$ . The  $D_s^+ \rightarrow K^0$  hadronic form factor is determined from the differential decay rate of  $D_s^+ \rightarrow K^0 e^+ \nu_e$  to be  $f_+^{K^0}(0) = 0.636 \pm 0.049 \pm 0.013$ . For both measurements, the first uncertainty is statistical and the second systematic. The branching fraction and form factor measurements are factors of 1.6 and 1.7 more precise than the previous world averages, respectively.

## I. INTRODUCTION

Studies of semileptonic  $D_s^+$  decays provide important input to understand the effects of the strong and weak interactions in charmed meson decays [1]. The partial decay rates of the semileptonic decays  $D_s^+ \rightarrow P \ell^+ \nu_\ell$  ( $P$  denotes a pseudoscalar meson) are proportional to the product of the hadronic form factor  $f_+^P(0)$  and the Cabibbo-Kobayashi-Maskawa (CKM) matrix element  $|V_{cs}|$  or  $|V_{cd}|$ . In recent years, there has been much

progress in the experimental study of semileptonic  $D_s^+$  decays. However, knowledge of Cabibbo-suppressed semileptonic  $D_s^+$  decays remains limited by statistical uncertainty [2]. Improved measurements of the branching fraction of  $D_s^+ \rightarrow K^0 e^+ \nu_e$  and the hadronic form factor of  $D_s^+ \rightarrow K^0$  are important to validate theoretical calculations [3–11]. The hadronic form factor measurement helps test and improve theoretical calculations, which in turn improves the measured precision of  $|V_{cd}|$ . This is important for testing the unitarity of the CKM matrix and searching for possible

indications of new physics.

Theoretical predictions of the branching fraction of  $D_s^+ \rightarrow K^0 e^+ \nu_e$  range from  $2.0 \times 10^{-3}$  to  $4.0 \times 10^{-3}$ . In 2009, the CLEO-c experiment reported the first measurement of the branching fraction of  $D_s^+ \rightarrow K^0 e^+ \nu_e$  using  $0.31 \text{ fb}^{-1}$  of  $e^+e^-$  collision data collected at a center-of-mass (CM) energy of 4.17 GeV [12]. In 2015, the CLEO collaboration updated the branching fraction measurement using  $0.586 \text{ fb}^{-1}$  of data at the same energy point [13]. In 2019, the BESIII experiment presented a further improved measurement of the branching fraction and the first measurement of the hadronic form factor in  $D_s^+ \rightarrow K^0 e^+ \nu_e$  by analyzing  $3.19 \text{ fb}^{-1}$  of data at 4.178 GeV [14, 15].

In this paper, we report improved measurements of both the branching fraction and the hadronic transition form factor in  $D_s^+ \rightarrow K^0 e^+ \nu_e$ , assuming  $K^0 \rightarrow K_S^0$  with a branching fraction of 50%, based on  $7.33 \text{ fb}^{-1}$  of  $e^+e^-$  collision data taken with center-of-mass (CM) energies between 4.128 and 4.226 GeV with the BESIII detector. Throughout this paper, charge conjugate modes are implied.

## II. BESIII DETECTOR AND MONTE CARLO SIMULATIONS

The BESIII detector [16] records symmetric  $e^+e^-$  collisions provided by the BEPCII storage ring [17], which operates with a peak luminosity of  $1.1 \times 10^{33} \text{ cm}^{-2}\text{s}^{-1}$  in the CM energy range from 1.84 to 4.95 GeV. BESIII has collected large data samples in this energy region [18]. The cylindrical core of the BESIII detector covers 93% of the full solid angle and consists of a helium-based multilayer drift chamber (MDC), a plastic scintillator time-of-flight system (TOF), and a CsI(Tl) electromagnetic calorimeter (EMC), all enclosed in a superconducting solenoidal magnet that provides a 1.0 T magnetic field. The solenoid is supported by an octagonal flux-return yoke with resistive plate counter muon identification modules interleaved with steel. The charged-particle momentum resolution at 1 GeV/c is 0.5%, and the  $dE/dx$  resolution is 6% for electrons from Bhabha scattering. The EMC measures photon energies with a resolution of 2.5% (5%) at 1 GeV in the barrel (end cap) region. The time resolution in the TOF barrel (end cap) region is 68 (110) ps, and the end cap TOF system was upgraded in 2015 using multi-gap resistive plate chamber technology, providing a time resolution of 60 ps [19]. Approximately 83% of the data benefits from this upgrade.

Simulated data samples produced with a GEANT4-based [20] Monte Carlo (MC) package, which includes the geometric description of the BESIII detector and the detector response, are used to determine detection efficiencies and to estimate backgrounds. The simulation models the beam energy spread and initial state radiation (ISR) in the  $e^+e^-$  annihilations with the generator

KKMC [21]. In the simulation, the production of open-charm processes directly produced via  $e^+e^-$  annihilations are modeled with the generator CONEXC [22], and their subsequent decays are modeled by EVTGEN [23] with known branching fractions from the Particle Data Group (PDG) [2]. The ISR production of vector charmonium(-like) states and the continuum processes are incorporated in KKMC [21]. The remaining unknown charmonium decays are modeled with LUNDCHARM [24]. Final state radiation (FSR) from charged final-state particles is incorporated using the PHOTOS package [25].

## III. ANALYSIS METHOD

Pairs of  $D_s^{*\pm} D_s^\mp$  decaying into  $\gamma D_s^+ D_s^-$  are produced copiously in  $e^+e^-$  collisions with CM energies between 4.128 and 4.226 GeV. This allows us to study  $D_s^+$  decays using the double-tag (DT) method pioneered by the MARK-III collaboration [26]. The  $D_s^-$  meson, which is fully reconstructed via one of its hadronic decay modes, is referred to as a single-tag (ST)  $D_s^-$  meson. In the presence of a fully reconstructed ST  $D_s^-$  meson at a certain CM energy, we can infer the kinematic information of the other  $D_s^+$  meson. The semileptonic decay  $D_s^+ \rightarrow K^0 e^+ \nu$  is thus selected on the side recoiling against the ST  $D_s^-$ , despite the presence of an undetectable neutrino. A DT event is an event in which the transition  $\gamma$  from the  $D_s^{*+}$  and the semileptonic decay  $D_s^+ \rightarrow K^0 e^+ \nu_e$  can be successfully selected in the presence of the ST. The branching fraction of  $D_s^+ \rightarrow K^0 e^+ \nu_e$  is determined by

$$\mathcal{B}_{D_s^+ \rightarrow K^0 e^+ \nu_e} = \frac{N_{\text{DT}}}{N_{\text{ST}}^{\text{tot}} \cdot \bar{\epsilon}_{\gamma\text{SL}}}, \quad (1)$$

where  $N_{\text{DT}} = \sum_{ij} N_{\text{DT}}^{ij}$  and  $N_{\text{ST}}^{\text{tot}} = \sum_{ij} N_{\text{ST}}^{ij}$  are the yields of the DT events and ST  $D_s^-$  mesons in data summing over all tag modes  $i$  and datasets  $j$ , respectively; and  $\bar{\epsilon}_{\gamma\text{SL}}$  is the efficiency of detecting the  $\gamma$  and the semileptonic decay in the presence of the ST  $D_s^-$  candidate, weighted by the ST yield in data. It is calculated by  $\sum_{ij} [(N^{ij}/N_{\text{ST}}) \cdot (\epsilon_{\text{DT}}^{ij}/\epsilon_{\text{ST}}^{ij})]$ , where  $\epsilon_{\text{DT}}^{ij}$  and  $\epsilon_{\text{ST}}^{ij}$  are the detection efficiencies of the DT and ST candidates, respectively.

## IV. SINGLE-TAG $D_s^-$ CANDIDATES

The ST  $D_s^-$  candidates are formed using fourteen hadronic decay modes:  $D_s^- \rightarrow K^+ K^- \pi^-$ ,  $K^+ K^- \pi^- \pi^0$ ,  $\pi^+ \pi^- \pi^-$ ,  $K_S^0 K^-$ ,  $K_S^0 K^- \pi^0$ ,  $K^- \pi^+ \pi^-$ ,  $K_S^0 K_S^0 \pi^-$ ,  $K_S^0 K^+ \pi^- \pi^-$ ,  $K_S^0 K^- \pi^+ \pi^-$ ,  $\eta_{\gamma\gamma} \pi^-$ ,  $\eta'_{\pi^+\pi^-} \rho^-$ ,  $\eta'_{\eta_{\gamma\gamma} \pi^+\pi^-} \pi^-$ ,  $\eta'_{\gamma\rho^0} \pi^-$ , and  $\eta_{\gamma\gamma} \rho^-$ . Throughout this paper, the subscripts on the  $\eta^{(\prime)}$  denote the decay modes that are used to reconstruct the  $\eta^{(\prime)}$  candidates and  $\rho$  denotes  $\rho(770)$ .

In selecting candidates for the  $K^\pm$ ,  $\pi^\pm$ ,  $K_S^0$ ,  $\gamma$ ,  $\pi^0$ , and  $\eta$ , we use the same selection criteria as those adopted in our previous works [28, 29]. All charged tracks, except for those from  $K_S^0$  decays, are required to originate from a region defined as  $|V_{xy}| < 1$  cm,  $|V_z| < 10$  cm, and  $|\cos\theta| < 0.93$ , where  $|V_{xy}|$  and  $|V_z|$  are the distances of closest approach to the interaction point (IP) in the transverse plane and along the MDC axis, respectively, and  $\theta$  is the polar angle with respect to the MDC axis. The particle identification (PID) of charged particles is performed with combined  $dE/dx$  and TOF information. Those with confidence level for the pion (kaon) hypothesis greater than that for the kaon (pion) hypothesis are assigned to be pion (kaon) candidates.

Candidates for  $K_S^0$  are reconstructed from two oppositely charged tracks satisfying  $|V_z| < 20$  cm. The two charged tracks are assigned as  $\pi^+\pi^-$  without imposing further PID criteria. They are constrained to originate from a common vertex and are required to have an invariant mass within  $|M_{\pi^+\pi^-} - m_{K_S^0}| < 12$  MeV/ $c^2$ , where  $m_{K_S^0}$  is the  $K_S^0$  nominal mass [2]. The decay length of the  $K_S^0$  candidate is required to be greater than twice the vertex resolution away from the IP.

Photon candidates are selected using information measured by the EMC and are required to satisfy the following criteria. To suppress backgrounds from electronic noise or bremsstrahlung, any candidate shower is required to start within [0, 700] ns from the event start time. The energy of each shower in the barrel (endcap) region of the EMC [16] is required to be greater than 25 (50) MeV. To suppress backgrounds associated with charged tracks, the minimum opening angle between the momentum of the candidate shower and the extrapolated momentum direction of the nearest charged track at the EMC has to be greater than  $10^\circ$ .

Candidates for  $\pi^0$  and  $\eta_{\gamma\gamma}$  are formed from  $\gamma\gamma$  pairs with invariant masses in the mass intervals (0.115, 0.150) and (0.50, 0.57) GeV/ $c^2$ , respectively. To improve momentum resolution, the invariant mass of each selected  $\gamma\gamma$  pair is constrained to either the  $\pi^0$  or  $\eta$  nominal mass [2]. To form candidates for  $\rho^{0(+)}$ ,  $\eta_{\pi^0\pi^+\pi^-}$ ,  $\eta_{\pi^+\pi^-}$ , and  $\eta'_{\gamma\rho^0}$ , the invariant masses of the  $\pi^+\pi^{-(0)}$ ,  $\pi^0\pi^+\pi^-$ ,  $\eta\pi^+\pi^-$ , and  $\gamma\rho^0$  combinations are required to be within the mass intervals of (0.57, 0.97), (0.53, 0.57), (0.946, 0.970), and (0.940, 0.976) GeV/ $c^2$ , respectively. In addition, the energy of the  $\gamma$  resulting from the  $\eta'_{\gamma\rho^0}$  decay is required to be greater than 0.1 GeV.

The background caused by the transition pions from  $D^{*+}$  decays is suppressed by requiring the momentum of any pion which is not from a  $K_S^0$ ,  $\eta$ , or  $\eta'$  to be greater than 0.1 GeV/ $c$ .

The backgrounds from non- $D_s^\pm D_s^{*\mp}$  processes are suppressed with the beam-constrained mass of the ST  $D_s^-$  candidate, which is defined as

$$M_{\text{BC}} \equiv \sqrt{E_{\text{beam}}^2/c^4 - |\vec{p}_{\text{tag}}|^2/c^2}, \quad (2)$$

where  $E_{\text{beam}}$  is the beam energy and  $\vec{p}_{\text{tag}}$  is the momentum of the ST  $D_s^-$  candidate in the  $e^+e^-$  CM frame. The  $M_{\text{BC}}$  is required to be within the intervals shown in Table 1. This requirement retains 90% of the  $D_s^-$  and  $D_s^+$  mesons from  $e^+e^- \rightarrow D_s^{*\mp} D_s^\pm$ .

Table 1. Requirements on  $M_{\text{BC}}$  for various energy points.

$E_{\text{CM}}$ (GeV)	$M_{\text{BC}}$ (GeV/ $c^2$ )
4.128	[2.010, 2.061]
4.157	[2.010, 2.070]
4.178	[2.010, 2.073]
4.189	[2.010, 2.076]
4.199	[2.010, 2.079]
4.209	[2.010, 2.082]
4.219	[2.010, 2.085]
4.226	[2.010, 2.088]

In the case of multiple candidates, only the candidate with the  $D_s^-$  recoil mass

$$M_{\text{rec}} \equiv \sqrt{\left(E_{\text{CM}}/c^2 - \sqrt{|\vec{p}_{\text{tag}}|^2/c^2 + m_{D_s^-}^2}\right)^2 - |\vec{p}_{\text{tag}}|^2/c^2} \quad (3)$$

closest to the  $D_s^{*+}$  nominal mass [2] per tag mode and per charge is retained for further analysis. The distributions of the invariant mass ( $M_{\text{tag}}$ ) of the accepted ST candidates for various tag modes are shown in Fig. 1. The yields of ST  $D_s^-$  mesons reconstructed in various tag modes are derived from fits to individual  $M_{\text{tag}}$  distributions and are listed in Table 2. In the fits, the signal is described by the simulated signal shape convolved with a Gaussian function that represents the resolution difference between data and simulation. In the fit to the  $D_s^- \rightarrow K_S^0 K^-$  tag mode, the shape of the peaking background from  $D^- \rightarrow K_S^0 \pi^-$  is modeled by the simulated shape convolved with the same Gaussian resolution function as the signal shape and the size of this peaking background is free. The combinatorial background is described by a second-order Chebychev polynomial function, and has been verified by analyzing the inclusive simulation sample. Figure 1 shows the results of the fit to the data sample. For each tag mode, the ST yield is obtained by integrating the signal shape over the selected  $D_s^-$  signal region defined within  $1.94 < M_{D_s^-} < 1.99$  GeV/ $c^2$ . The second and third columns of Table 2 summarize the yields of ST  $D_s^-$  mesons ( $N_{\text{ST}}$ ) for various tag modes obtained from the data sample and the corresponding detection efficiencies ( $\epsilon_{\text{ST}}$ ), respectively. The total ST yield summed over all ST modes is  $N_{\text{ST}}^{\text{tot}} = (783.1 \pm 2.5) \times 10^{-3}$ , where the uncertainty is statistical only.

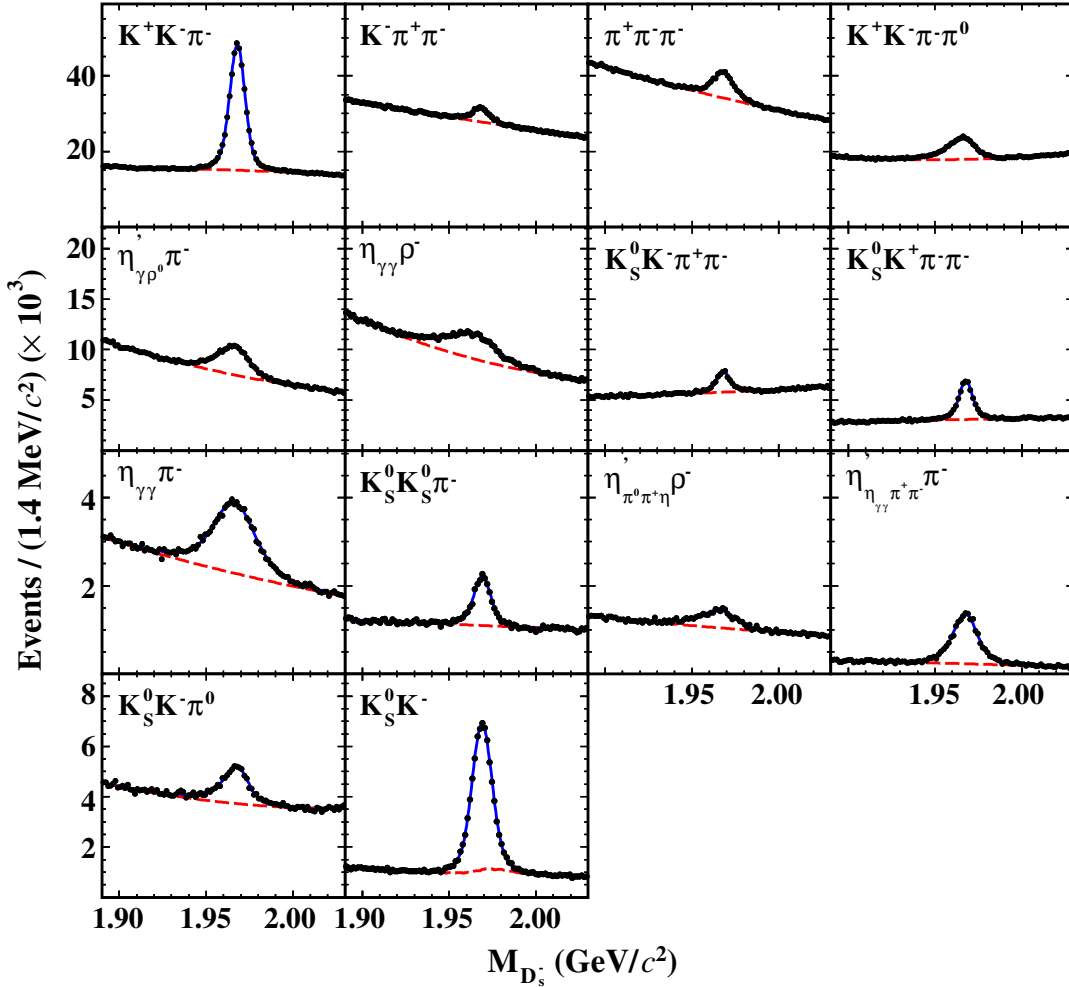


Fig. 1. Fits to the  $M_{D_s^-}$  distributions of the ST candidates for various tag modes. The points with error bars are data; the blue solid curves are the best fit results; and the red dashed curves are the fitted background shapes.

### V. SELECTION OF $D_s^+ \rightarrow K^0 e^+ \nu_e$

In the system recoiling against the  $D_s^-$  tag and the transition  $\gamma$  from the  $D_s^{*-}$ , the semileptonic decay  $D_s^+ \rightarrow K^0 e^+ \nu_e$  is selected using tracks that have not been used for the single tag reconstruction. To identify positrons, the combined confidence levels  $CL'_e$ ,  $CL'_\pi$ , and  $CL'_K$  for the electron, pion, and kaon hypotheses are calculated with the  $dE/dx$ , TOF, and EMC information. The positron candidates are required to satisfy  $CL'_e > 0.001$  and  $CL'_e / (CL'_e + CL'_\pi + CL'_K) > 0.8$ .

The background from  $D_s^+ \rightarrow K^0 K^+$  is vetoed by requiring the  $K^0 e^+$  invariant mass to be less than  $1.78 \text{ GeV}/c^2$ . The background contributions from  $D_s^+$  hadronic decays associated with fake photons misidentified from showers are rejected by requiring the largest energy of the unused showers ( $E_{\text{extra}\gamma}^{\text{max}}$ ) to be less than  $0.2 \text{ GeV}$ .

To identify the transition  $\gamma$  produced directly from the  $D_s^{\pm}$ , we perform kinematic fits under two hypotheses. One assumes that the  $D_s^{*-}$  is formed by the transition

$\gamma$  and the ST  $D_s^-$ , and the other assumes that the  $D_s^{*+}$  is formed by the transition  $\gamma$  and the semileptonic decay. The final particles from the  $D_s^{\mp} D_s^{\pm}$  system are constrained to obey energy and momentum conservation in the  $e^+ e^-$  CM frame with the neutrino treated as a missing particle. The particle candidates for  $D_s^{\pm}$  are constrained to their known mass from the PDG [2]. For the former hypothesis, the mass of the transition  $\gamma$  and the tagged  $D_s^-$  is constrained to the known  $D_s^{*-}$  mass. For the latter hypothesis, the mass of the transition  $\gamma$  and the semileptonic decay is constrained to the known  $D_s^{*+}$  mass. The hypothesis with the smallest  $\chi^2$  of the kinematic fit ( $\chi_{\text{KMFIT}}^2$ ), which also satisfies  $\chi_{\text{KMFIT}}^2 < 100$ , is kept for further analysis.

The presence of the neutrino is inferred from the distribution of the missing-mass squared variable, which is defined as

$$M_{\text{miss}}^2 = E_{\text{miss}}^2/c^4 - |\vec{p}_{\text{miss}}|^2/c^2. \quad (4)$$

Here,  $E_{\text{miss}} = E_{\text{CM}} - \sum_i E_i$  and  $\vec{p}_{\text{miss}} = \sum_i \vec{p}_i$ , where  $E_i$

Table 2. Fitted yields of single-tag  $D_s^-$  mesons from the data sample ( $N_{\text{ST}}$ ), the efficiencies of detecting single-tag  $D_s^-$  mesons and double-tag events ( $\epsilon_{\text{ST}}$  and  $\epsilon_{\text{DT}}$ ) for various tag modes. For all quantities, the uncertainties are statistical only. The listed efficiencies do not include the branching fractions of the daughter particles's decays.

Tag mode	$N_{\text{ST}} (\times 10^3)$	$\epsilon_{\text{ST}} (\%)$	$\epsilon_{\text{DT}} (\%)$
$K^+ K^- \pi^-$	$281.7 \pm 0.8$	$41.94 \pm 0.03$	$10.92 \pm 0.11$
$K^+ K^- \pi^- \pi^0$	$85.4 \pm 1.0$	$11.53 \pm 0.03$	$3.39 \pm 0.12$
$\pi^- \pi^+ \pi^-$	$76.9 \pm 1.0$	$53.84 \pm 0.06$	$15.28 \pm 0.11$
$K_S^0 K^-$	$63.2 \pm 0.3$	$47.18 \pm 0.06$	$12.73 \pm 0.11$
$K_S^0 K^- \pi^0$	$21.9 \pm 0.5$	$16.56 \pm 0.08$	$4.81 \pm 0.12$
$K^- \pi^+ \pi^-$	$36.8 \pm 0.8$	$47.06 \pm 0.08$	$12.78 \pm 0.11$
$K_S^0 K_S^0 \pi^-$	$10.6 \pm 0.2$	$22.92 \pm 0.13$	$5.82 \pm 0.12$
$K_S^0 K^+ \pi^- \pi^-$	$30.5 \pm 0.3$	$21.48 \pm 0.07$	$5.48 \pm 0.12$
$K_S^0 K^- \pi^+ \pi^-$	$16.4 \pm 0.4$	$19.21 \pm 0.10$	$4.74 \pm 0.12$
$\eta \pi^-$	$33.7 \pm 0.6$	$40.43 \pm 0.08$	$12.54 \pm 0.11$
$\eta'(\pi^+ \pi^- \eta) \rho^-$	$7.2 \pm 0.3$	$5.62 \pm 0.08$	$1.83 \pm 0.11$
$\eta'(\eta \pi^+ \pi^-) \pi^-$	$15.6 \pm 0.2$	$19.20 \pm 0.10$	$5.45 \pm 0.12$
$\eta'(\gamma \rho) \pi^-$	$47.3 \pm 0.7$	$30.94 \pm 0.07$	$8.77 \pm 0.11$
$\eta \rho^-$	$56.0 \pm 1.2$	$14.35 \pm 0.04$	$5.02 \pm 0.12$

and  $\vec{p}_i$ , with  $i = (\text{tag}, \gamma, e, \text{ and } K^0)$ , are the energy and momentum of particle  $i$ .

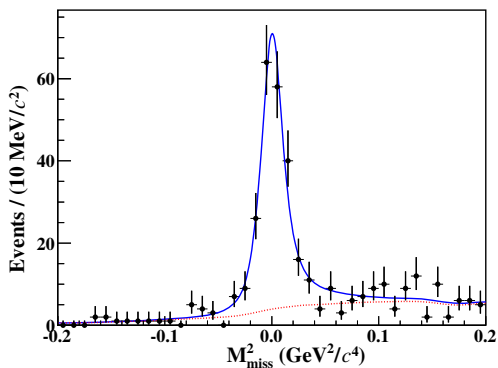


Fig. 2. Fit to the  $M_{\text{miss}}^2$  distribution of the candidates for  $D_s^+ \rightarrow K^0 e^+ \nu_e$ . The points with error bars are the data summed over all CM energies; the blue solid curve is the total fit; and the red dashed curve is the fitted background shape.

The  $M_{\text{miss}}^2$  distribution of the accepted candidates for  $D_s^+ \rightarrow K^0 e^+ \nu_e$  in data summed over all CM energies is shown in Fig. 2. The signal yield of  $D_s^+ \rightarrow K^0 e^+ \nu_e$  ( $N_{\text{DT}}$ ) is derived from an unbinned maximum likelihood fit to this distribution. In this fit, the signal is described by a simulated signal shape convolved with a Gaussian function with free parameters to compensate for the resolution difference between data and MC simulation. The background is described by a simulated shape derived from the inclusive MC sample. From this fit, the signal yield is  $225.3 \pm 17.3$  where the uncertainty is

statistical only. The corresponding DT efficiencies  $\epsilon_{\text{DT}}^i$  of various ST are summarized in the fourth column of Table 2.

## VI. BRANCHING FRACTION

The detection efficiency  $\epsilon_{\text{SL}}$ , which does not include the branching fraction of  $K^0 \rightarrow K_S^0 \rightarrow \pi^+ \pi^-$ , is estimated to be  $(27.88 \pm 0.21)\%$  for  $D_s^+ \rightarrow K^0 e^+ \nu_e$ . Figure 3 shows good consistency in the  $\cos\theta$  and momenta distributions for the  $K^0$  and  $D_s^+ \rightarrow K^0 e^+ \nu_e$  candidates between data and the inclusive MC sample. The branching fraction of  $D_s^+ \rightarrow K^0 e^+ \nu_e$  is determined by Eq. (1) to be

$$\mathcal{B}(D_s^+ \rightarrow K^0 e^+ \nu_e) = (2.98 \pm 0.23 \pm 0.12) \times 10^{-3},$$

where the first uncertainty is statistical and the second is systematic, which is discussed below and summarized in Table 3.

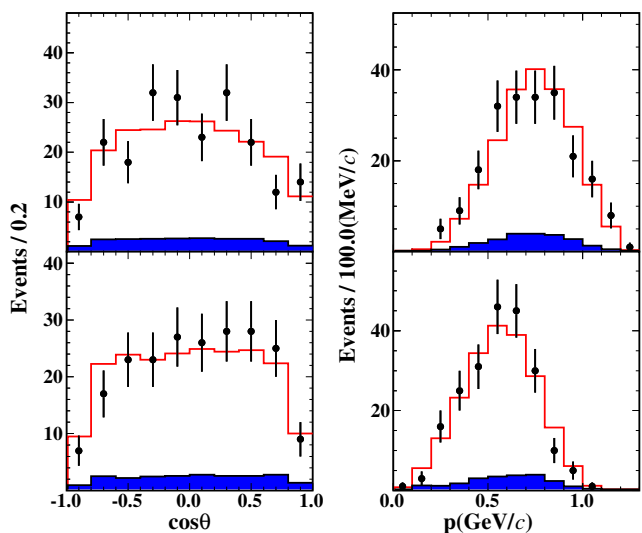


Fig. 3. Comparison of  $\cos\theta$  and momenta for the  $K^0$  (top) and candidates for  $D_s^+ \rightarrow K^0 e^+ \nu_e$  (bottom) using all CM energies between 4.128 and 4.226 GeV. The points with error bars are data; the blue filled histograms are the simulated background; and the red line histograms are the inclusive MC samples. These events have been required to satisfy  $|M_{\text{miss}}^2| < 0.03 \text{ GeV}^2/c^4$ .

Our measurement is performed using the DT technique [26], and most systematic uncertainties related to the ST selection criteria therefore cancel. The systematic uncertainty of the ST  $D_s^-$  yields is evaluated to be 1.0% by using alternative signal and background shapes in the fits to the  $M_{\text{tag}}$  spectra. The systematic uncertainty for the  $e^\pm$  tracking and PID efficiency is 1.0% each, and is studied using a control sample of  $e^+ e^- \rightarrow \gamma e^+ e^-$  [32]. The systematic uncertainty in the  $K_S^0$  reconstruction efficiency is estimated with the control samples  $J/\psi \rightarrow K^*(892)^\mp K^\pm$  and  $J/\psi \rightarrow \phi K_S^0 K^\pm \pi^\mp$  [33] and is determined to be 1.5% per



$K_S^0$ . The systematic uncertainty of the transition  $\gamma$  reconstruction [34], which is weighted by the branching fraction of  $D_s^{*+} \rightarrow \gamma D_s^+$ , is assigned to be 1.0%. The systematic uncertainties due to the requirements of  $E_{\text{extra}}^{\text{max}}$  and  $\chi_{\text{KMFIT}}^2$  are estimated using the control samples  $D_s^+ \rightarrow K_S^0 K^+$  and  $D_s^+ \rightarrow K_S^0 K^+ \pi^0$ . The differences of the acceptance efficiencies between data and MC simulation, 0.8% and 2.3%, are assigned as individual systematic uncertainties. The systematic uncertainty due to the different tag dependence between data and MC simulation, called the tag bias [32], is estimated to be 0.2%. The systematic uncertainty of the quoted branching fraction of  $K^0 \rightarrow K_S^0 \rightarrow \pi^+ \pi^-$  is 0.1% [2]. The systematic uncertainty arising from the fit to the  $M_{\text{miss}}^2$  distribution is estimated to be 0.9% by varying the signal and background shapes. The uncertainty due to MC statistics is 0.2%. Systematic uncertainty due to the uncertainty on the form factor used in the MC simulation to determine the efficiency is estimated to be 1.4%. This is evaluated by comparing the difference of the signal efficiencies when varying the input hadronic form factor parameter by  $\pm 1\sigma$ , as determined in this work listed in Table 8. Adding these effects in quadrature, we obtain the total systematic uncertainty on the measurement of the branching fraction of  $D_s^+ \rightarrow K^0 e^+ \nu_e$  to be 3.9%. A summary of the systematic uncertainties for the branching fraction is shown in Table 3.

Table 3. Sources of systematic uncertainties in the branching fraction measurement.

Source	Uncertainty (%)
Single-tag yield	1.0
$e^+$ tracking	1.0
$e^+$ PID	1.0
$K_S^0$ reconstruction	1.5
Transition $\gamma$ reconstruction	1.0
$E_{\text{extra}}^{\text{max}}$ $\gamma$ and $N_{\text{extra}}^{\text{charge}}$ requirements	0.8
$\chi_{\text{KMFIT}}^2$ requirement	2.3
Tag bias	0.2
Quoted branching fraction	0.1
$M_{\text{miss}}^2$ fit	0.9
MC statistics	0.2
Hadronic form factor	1.4
Total	3.9

## VII. HADRONIC FORM FACTOR

To study the decay dynamics of the semileptonic decay  $D_s^+ \rightarrow K^0 e^+ \nu_e$ , candidates are divided according to the invariant mass squared of the  $e^+ \nu_e$  system ( $q^2 = (E_e/c + E_\nu/c)^2 + |\vec{p}_e + \vec{p}_\nu|^2$ ) into five intervals (0.00, 0.35], (0.35, 0.70], (0.70, 1.05], (1.05, 1.40] and

Table 4. Efficiency matrix (in %) for  $D_s^+ \rightarrow K^0 e^+ \nu_e$ . The efficiencies do not include the branching fractions of the decays of the daughter particles.

$(i, j)$ $q^2$ interval	1	2	3	4	5
1	26.80	0.83	0.00	0.00	0.00
2	0.93	27.62	0.74	0.02	0.00
3	0.00	0.91	27.09	0.64	0.00
4	0.00	0.00	0.83	26.12	0.41
5	0.00	0.00	0.00	0.70	25.56

(1.40, 2.16)  $\text{GeV}^2/c^4$ . The partial decay rate in the  $i$ th  $q^2$  interval,  $\Delta\Gamma_{\text{measured}}^i$ , is determined by

$$\Delta\Gamma_{\text{measured}}^i = N_{\text{produced}}^i / (\tau_{D_s^+} \mathcal{B}_{K^0 \rightarrow \pi^+ \pi^-} N_{\text{ST}}^{\text{tot}}), \quad (5)$$

where  $N_{\text{produced}}^i$  is the  $D_s^+ \rightarrow K^0 e^+ \nu_e$  signal yield produced in the  $i$ th  $q^2$  interval in data,  $\tau_{D_s^+}$  is the lifetime of the  $D_s^+$  [2], and  $N_{\text{ST}}^{\text{tot}}$  is the total yield of ST  $D_s^-$  mesons. The number of events produced in data is calculated as

$$N_{\text{produced}}^i = \sum_j^{N_{\text{intervals}}} (\varepsilon^{-1})_{ij} N_{\text{observed}}^j, \quad (6)$$

where  $N_{\text{observed}}^j$  is the  $D_s^+ \rightarrow K^0 e^+ \nu_e$  signal yield observed in the  $j$ th  $q^2$  interval and  $\varepsilon$  is the efficiency matrix, which also includes the effects of bin migration, given by

$$\varepsilon_{ij} = \sum_k \left[ (N_{\text{reconstructed}}^{ij} \cdot N_{\text{ST}}) / (N_{\text{generated}}^j \cdot \varepsilon_{\text{ST}}) \right]_k / N_{\text{ST}}^{\text{tot}}. \quad (7)$$

Here,  $N_{\text{reconstructed}}^{ij}$  is the  $D_s^+ \rightarrow K^0 e^+ \nu_e$  signal yield generated in the  $j$ th  $q^2$  interval and reconstructed in the  $i$ th  $q^2$  interval,  $N_{\text{generated}}^j$  is the total signal yield generated in the  $j$ th  $q^2$  interval, and the index  $k$  sums over all tag modes and energies.

The signal yield  $N_{\text{observed}}^i$  in each  $q^2$  interval is obtained from the fit to the corresponding  $M_{\text{miss}}^2$  distribution, and is shown in Fig. 4. The efficiency matrix for  $D_s^+ \rightarrow K^0 e^+ \nu_e$  is shown in Table 4. The values for  $N_{\text{observed}}^j$ ,  $N_{\text{produced}}^j$ ,  $\Delta\Gamma_j$ , and  $\frac{\Delta\Gamma_j}{\Delta q_j^2}$  are summarized in Table 5.

Using the values of  $\Delta\Gamma_{\text{measured}}^i$  obtained above and the theoretical parameterization of the partial decay rate  $\Delta\Gamma_{\text{expected}}^i$  described below, form factor parameters are extracted by a  $\chi^2$  fit where the  $\chi^2$  is constructed as

$$\chi^2 = \sum_{i,j=1}^5 \left( \Delta\Gamma_{\text{measured}}^i - \Delta\Gamma_{\text{expected}}^i \right) C_{ij}^{-1} \left( \Delta\Gamma_{\text{measured}}^j - \Delta\Gamma_{\text{expected}}^j \right), \quad (8)$$

where  $C_{ij} = C_{ij}^{\text{stat}} + C_{ij}^{\text{syst}}$  is the covariance matrix of the

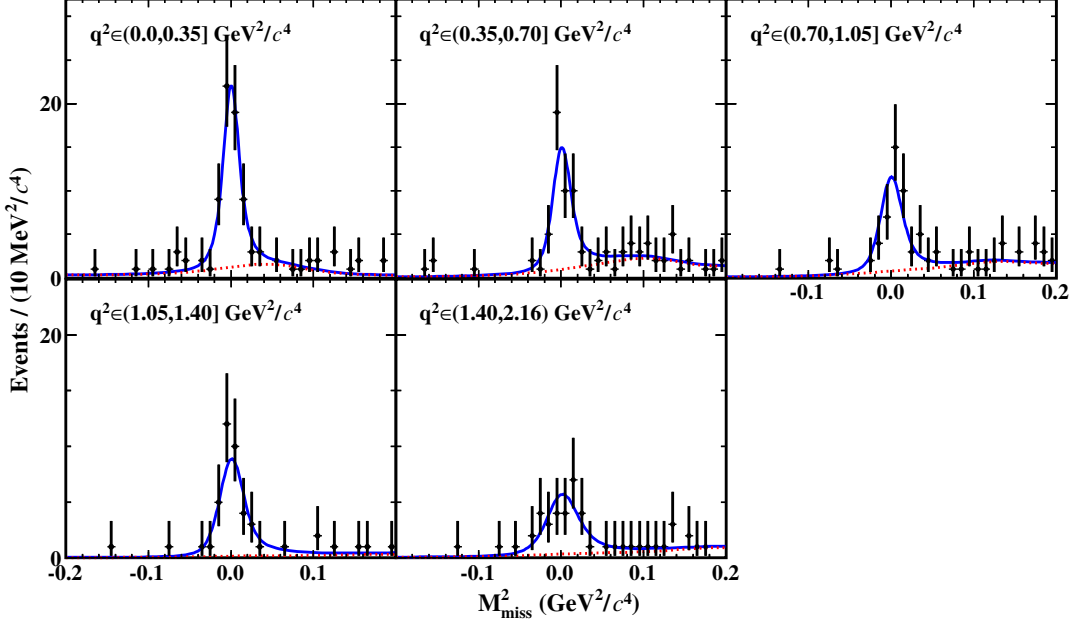


Fig. 4. Fits to the  $M_{\text{miss}}^2$  distributions of  $D_s^+ \rightarrow K^0 e^+ \nu_e$  in various reconstructed  $q^2$  intervals. The points with error bars are the data summed over all CM energies; the blue solid curves are the best fits; and the red dashed curves are the fitted background shapes.

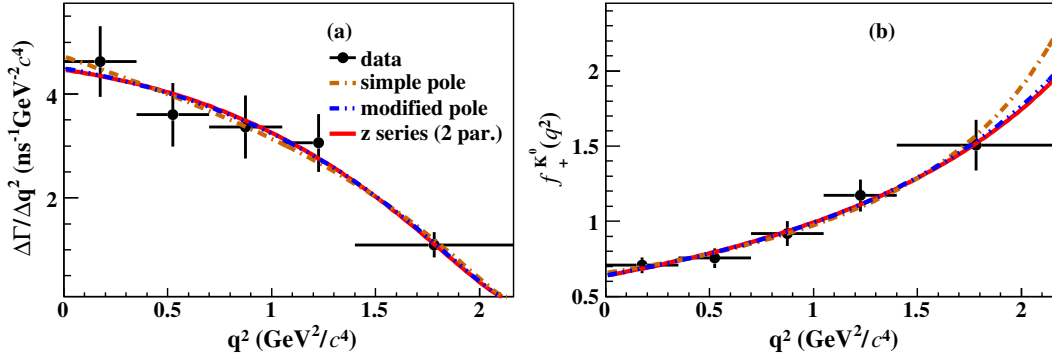


Fig. 5. (a) Fit to the partial decay width of  $D_s^+ \rightarrow K^0 e^+ \nu_e$  and (b) projection to the hadronic form factor as a function of  $q^2$ . The points with error bars are the measured partial decay widths, where the horizontal and vertical errors represent the  $q^2$  bin interval and the error of the corresponding partial decay width, respectively. The solid red curves are the best fits.

measured partial decay rates among  $q^2$  intervals. The differential decay rate is given by

$$\frac{d\Gamma(D_s^+ \rightarrow K^0 e^+ \nu_e)}{dq^2} = \frac{G_F^2 |V_{cd}|^2}{24\pi^3} p_{K^0}^3 |f_+^{K^0}(q^2)|^2, \quad (9)$$

where  $p_{K^0}$  is the  $K^0$  momentum in the rest frame of the  $D_s^+$ ,  $G_F$  is the Fermi coupling constant [2],  $|V_{cd}|$  is the  $c \rightarrow d$  CKM matrix element, and  $f_+^{K^0}(q^2)$  is the hadronic form factor. The scalar hadronic form factor  $f_0^{K^0}(q^2)$  has been ignored because it is proportional to the positron mass squared.

The hadronic form factor,  $f_+^{K^0}(q^2)$ , is usually parameterized by the simple pole model, modified pole

model, or series expansion. In the modified pole model [30],

$$f_+^{K^0}(q^2) = \frac{f_+^{K^0}(0)}{(1 - \frac{q^2}{M_{\text{pole}}^2})(1 - \alpha \frac{q^2}{M_{\text{pole}}^2})}, \quad (10)$$

where  $M_{\text{pole}}$  is fixed to the known  $D^{*+}$  mass and  $\alpha$  is a free parameter. Setting  $\alpha = 0$  and leaving  $M_{\text{pole}}$  free, the simple pole model is recovered [31]. Due to limited statistics, we adopt the two parameter series expansion

Table 5. Partial decay rates of  $D_s^+ \rightarrow K^0 e^+ \nu_e$  in various  $q^2$  intervals of data, where the uncertainties are statistical only.

$q^2$ interval	(0.0,0.35]	(0.35,0.70]	(0.70,1.05]	(1.05,1.40]	(1.40,2.16]
$N_{\text{observed}}^j$	$60.7 \pm 8.7$	$50.8 \pm 8.1$	$46.1 \pm 7.8$	$40.0 \pm 6.7$	$30.2 \pm 6.5$
$N_{\text{produced}}^i$	$221.1 \pm 32.5$	$172.2 \pm 29.4$	$169.9 \pm 28.9$	$146.2 \pm 26.5$	$114.1 \pm 25.4$
$\Delta\Gamma_i$ (ns $^{-1}$ )	$1.62 \pm 0.24$	$1.26 \pm 0.22$	$1.18 \pm 0.21$	$1.07 \pm 0.19$	$0.84 \pm 0.19$
$\frac{\Delta\Gamma_i}{\Delta q_i^2}$ (ns $^{-1}$ GeV $^{-2}$ c $^4$ )	$4.63 \pm 0.68$	$3.60 \pm 0.62$	$3.37 \pm 0.60$	$3.06 \pm 0.55$	$1.10 \pm 0.24$

form, which is written as

$$f_+^{K^0}(q^2) = \frac{f_+^{K^0}(0)P(0)\Phi(0, t_0)}{P(q^2)\Phi(q^2, t_0)} \cdot \frac{1 + r_1(t_0)z(q^2, t_0)}{1 + r_1(t_0)z(0, t_0)}, \quad (11)$$

where  $t_0 = t_+(1 - \sqrt{1 - t_-/t_+})$ ,  $t_{\pm} = (m_{D_s^{\pm}} \pm m_{K^0})^2$ , and the functions  $P(q^2)$ ,  $\Phi(q^2, t_0)$ , and  $z(q^2, t_0)$  are defined following Ref. [31].

The statistical covariance matrix is constructed as

$$C_{ij}^{\text{stat}} = \left( \frac{1}{\tau_{D_s^+} \cdot N_{\text{ST}}^{\text{tot}}} \right)^2 \sum_n \varepsilon_{in}^{-1} \varepsilon_{jn}^{-1} (\sigma(N_{\text{obs}}^n))^2, \quad (12)$$

where  $n$  labels the  $q^2$  interval and the sum extends from 1 to 5. The systematic covariance matrix is obtained by summing over the covariance matrix of each systematic uncertainty source. This is taken as

$$C_{ij}^{\text{syst}} = \delta(\Delta\Gamma_{\text{measured}}^i) \delta(\Delta\Gamma_{\text{measured}}^j), \quad (13)$$

where  $\delta(\Delta\Gamma_{\text{measured}}^i)$  is the systematic uncertainty of the partial decay rate in the  $i$ th  $q^2$  interval. The systematic uncertainties due to  $\tau_{D_s^+}$ ,  $N_{\text{ST}}^{\text{tot}}$ ,  $e^+$  tracking efficiency,  $e^+$  PID efficiency,  $K_S^0$  reconstruction efficiency, transition  $\gamma$  reconstruction,  $\chi_{\text{KMFIT}}^2$  requirement, quoted branching fraction, and  $E_{\text{extra}}^{\text{max}}$  and  $N_{\text{extra}}^{\text{charge}}$  requirements are taken to be common across all the  $q^2$  intervals. The other systematic uncertainties in the branching fraction measurement, as shown in Table 3, are determined separately in various  $q^2$  intervals. The resulting statistical and systematic correlation coefficients are summarized in Tables 6 and 7, respectively.

Table 6. The statistical correlation coefficients of the measured partial decay rate in each  $q^2$  bin for  $D_s^+ \rightarrow K^0 e^+ \nu_e$ .

$\epsilon_{ij}$	1	2	3	4	5
1	1.000	-0.065	0.003	-0.000	0.000
2	-0.065	1.000	-0.060	0.003	-0.000
3	0.003	-0.060	1.000	-0.057	0.002
4	-0.000	0.003	-0.057	1.000	-0.044
5	0.000	-0.000	0.020	-0.044	1.000

Minimizing the  $\chi^2$  constructed in Eq. (8), we obtain the product,  $f_+^{K^0}(0)|V_{cd}|$ , and the parameters of various hadronic form factor parameterizations. The obtained

Table 7. The systematic correlation coefficients of the measured partial decay rate in each  $q^2$  bin for  $D_s^+ \rightarrow K^0 e^+ \nu_e$ .

$\epsilon_{ij}$	1	2	3	4	5
1	1.000	0.920	0.814	0.952	0.590
2	0.920	1.000	0.816	0.844	0.706
3	0.814	0.816	1.000	0.782	0.893
4	0.952	0.844	0.782	1.000	0.519
5	0.590	0.706	0.893	0.519	1.000

results are summarized in Table 8 and the fit results are shown in Fig. 5. The nominal fit parameters are taken from the fit with the combined statistical and systematic covariance matrix, and their statistical uncertainties are taken from the fit with the statistical covariance matrix. For each parameter, the systematic uncertainty is obtained by calculating the quadratic difference of uncertainties between these two fits. Taking the CKM matrix element  $|V_{cd}| = 0.22486 \pm 0.00067$  [2] as input, we obtain  $f_+^{K^0}(0)$  as summarized in the last column of Table 8, where the first uncertainties are statistical and the second are systematic.

## VIII. SUMMARY

In summary, using 7.33 fb $^{-1}$  of  $e^+e^-$  collision data taken between 4.128 and 4.226 GeV with the BESIII detector, the branching fraction of  $D_s^+ \rightarrow K^0 e^+ \nu_e$  is measured to be  $(2.98 \pm 0.23 \pm 0.12) \times 10^{-3}$ , where the first uncertainty is statistical and the second is the systematic. To measure the hadronic form factor at maximum recoil in  $D_s^+ \rightarrow K^0 e^+ \nu_e$ , we use the two parameter  $z$  series expansion. Based on the fit to the  $D_s^+ \rightarrow K^0 e^+ \nu_e$  partial decay rates in intervals of  $q^2$ , we measure  $f_+^{K^0}(0) = 0.636 \pm 0.049 \pm 0.013$ . Figure 6 compares the measured branching fraction and the hadronic form factor in  $D_s^+ \rightarrow K^0 e^+ \nu_e$  with theoretical calculations and other experiments. The precision of the measurements are improved by factors of 1.6 and 1.7, respectively, compared to the previous BESIII result [14]. The results can test various theoretical calculations.

Table 8. Hadronic form factors of  $D_s^+ \rightarrow K^0 e^+ \nu_e$ , where the first uncertainties are statistical and the second systematic. The parameter for the two-parameter  $z$  series expansion is  $r_1$  and the coefficient between the two fitted parameters is given in the fourth column. The  $\chi^2/\text{NDOF}$  is the goodness-of-fit and NDOF is the number of degrees of freedom.

Parametrization	$f_+^{K^0}(0) V_{cd} $	Parameter ( $M_{\text{pole}}^2/\alpha/r_1$ )	Coefficient	$\chi^2/\text{NDOF}$	$f_+^{K^0}(0)$
Simple pole [30]	$0.147 \pm 0.009 \pm 0.001$	$1.75 \pm 0.09 \pm 0.03$	0.72	0.96/3	$0.654 \pm 0.040 \pm 0.004$
Modified pole [30]	$0.144 \pm 0.010 \pm 0.002$	$0.57 \pm 0.25 \pm 0.08$	-0.81	0.93/3	$0.640 \pm 0.044 \pm 0.009$
$z$ series (two par.) [31]	$0.143 \pm 0.011 \pm 0.003$	$-3.7 \pm 1.5 \pm 0.5$	0.85	0.97/3	$0.636 \pm 0.049 \pm 0.013$

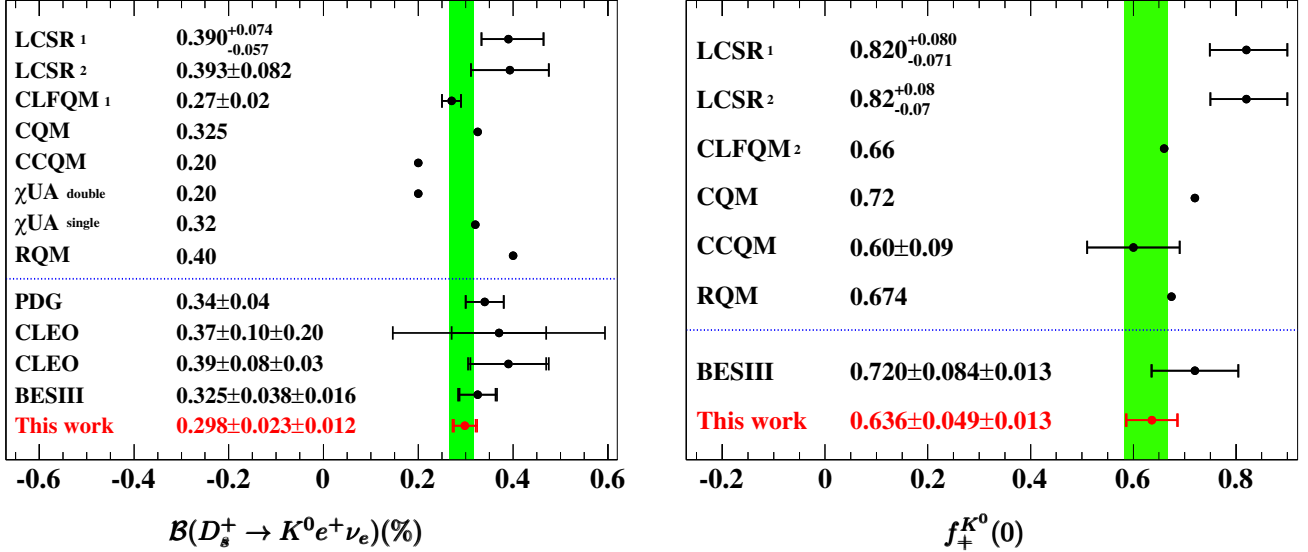


Fig. 6. Comparison of the measured branching fraction of  $D_s^+ \rightarrow K^0 e^+ \nu_e$  (left) and the hadronic form factor (right) of  $D_s^+ \rightarrow K^0$  with theoretical calculations and other experiments. The data in the comparison come from LCSR<sub>1</sub> [3], LCSR<sub>2</sub> [4], CLFQM<sub>1</sub> [5], CLFQM<sub>2</sub> [6], CQM [7], CCQM [8, 9],  $\chi\text{UA}_{\text{double pole}}$  [10],  $\chi\text{UA}_{\text{single pole}}$  [10], RQM [11], PDG [2], CLEO [12], CLEO [13], and BESIII [14].

## IX. ACKNOWLEDGEMENT

The BESIII Collaboration thanks the staff of BEPCII and the IHEP computing center for their strong support. This work is supported in part by National Key R&D Program of China under Contracts Nos. 2020YFA0406400, 2023YFA1606000, 2020YFA0406300; National Natural Science Foundation of China (NSFC) under Contracts Nos. 11635010, 11735014, 11935015, 11935016, 11935018, 12025502, 12035009, 12035013, 12061131003, 12192260, 12192261, 12192262, 12192263, 12192264, 12192265, 12221005, 12225509, 12235017, 12361141819; the Chinese Academy of Sciences (CAS) Large-Scale Scientific Facility Program; the CAS Center for Excellence in Particle Physics (CCEPP); Joint Large-Scale Scientific Facility Funds of the NSFC and CAS under Contract No. U1832207; 100 Talents Program of CAS; The Institute of Nuclear and Particle Physics

(INPAC) and Shanghai Key Laboratory for Particle Physics and Cosmology; German Research Foundation DFG under Contracts Nos. 455635585, FOR5327, GRK 2149; Istituto Nazionale di Fisica Nucleare, Italy; Knut and Alice Wallenberg Foundation under Contracts Nos. 2021.0174, 2021.0299; Ministry of Development of Turkey under Contract No. DPT2006K-120470; National Research Foundation of Korea under Contract No. NRF-2022R1A2C1092335; National Science and Technology fund of Mongolia; National Science Research and Innovation Fund (NSRF) via the Program Management Unit for Human Resources & Institutional Development, Research and Innovation of Thailand under Contract No. B16F640076; Polish National Science Centre under Contract No. 2019/35/O/ST2/02907; The Swedish Research Council; U. S. Department of Energy under Contract No. DE-FG02-05ER41374

[1] H. B. Li and X. R. Lyu, *Natl. Sci. Rev.* **8** 11, nwab181 (2021).

[2] R. L. Workman *et al.* (Particle Data Group), *Prog. Theor. Exp. Phys.* **2022**, 083C01 (2022).

- [3] Y. L. Wu, M. Zhong, and Y. B. Zuo, *Int. J. Mod. Phys. A* **21**, 6125 (2006).
- [4] X. Leng, X. L. Mu, Z. T. Zou, and Ying Li, *Chin. Phys. C* **45**, 063107 (2021).
- [5] H. Y. Cheng and X. W. Kang, *Eur. Phys. J. C* **77**, 587 (2017); **77**, 863(E) (2017).
- [6] R. C. Verma, *J. Phys. G* **39**, 025005 (2012).
- [7] D. Melikhov and B. Stech, *Phys. Rev. D* **62**, 014006 (2000).
- [8] N. R. Soni, M. A. Ivanov, J. G. Körner, J. N. Pandya, P. Santorelli, and C. T. Tran, *Phys. Rev. D* **98**, 114031 (2018).
- [9] M. A. Ivanov, J. G. Körner, J. N. Pandya, P. Santorelli, N. R. Soni, and C. T. Tran, *Front. Phys. (Beijing)* **14**, 64401 (2019).
- [10] S. Fajfer and J. Kamenik, *Phys. Rev. D* **71**, 014020 (2005).
- [11] R. N. Faustov, V. O. Galkin, and X. W. Kang, *Phys. Rev. D* **101**, 013004 (2020).
- [12] J. Yelton *et al.* (CLEO Collaboration), *Phys. Rev. D* **80**, 052007 (2009).
- [13] J. Hietala, D. Cronin-Hennessy, T. Pedlar, and I. Shipsey, *Phys. Rev. D* **92**, 012009 (2015).
- [14] M. Ablikim *et al.* (BESIII Collaboration), *Phys. Rev. Lett.* **122**, 061801 (2019).
- [15] B. C. Ke, J. Koponen, H. B. Li and Y. Zheng, *Ann. Rev. Nucl. Part. Sci.* **73**, 285-314 (2023).
- [16] M. Ablikim *et al.* (BESIII Collaboration), *Nucl. Instrum. Meth. A* **614**, 345 (2010).
- [17] C. H. Yu *et al.*, *Proceedings of IPAC2016, Busan, Korea, 2016*.
- [18] M. Ablikim *et al.* (BESIII Collaboration), *Chin. Phys. C* **44**, 040001 (2020).
- [19] X. Li *et al.*, *Radiat. Detect. Technol. Methods* **1**, 13 (2017); Y. X. Guo *et al.*, *Radiat. Detect. Technol. Methods* **1**, 15 (2017); P. Cao *et al.*, *Nucl. Instrum. Meth. A* **953**, 163053 (2020).
- [20] S. Agostinelli *et al.* (GEANT4 Collaboration), *Nucl. Instrum. Meth. A* **506**, 250 (2003).
- [21] S. Jadach, B. F. L. Ward and Z. Was, *Phys. Rev. D* **63**, 113009 (2001); *Comput. Phys. Commun.* **130**, 260 (2000).
- [22] R. G. Ping, *Chin. Phys. C* **38**, 083001 (2014);
- [23] D. J. Lange, *Nucl. Instrum. Meth. A* **462**, 152 (2001); R. G. Ping, *Chin. Phys. C* **32**, 599 (2008).
- [24] J. C. Chen, G. S. Huang, X. R. Qi, D. H. Zhang and Y. S. Zhu, *Phys. Rev. D* **62**, 034003 (2000); R. L. Yang, R. G. Ping and H. Chen, *Chin. Phys. Lett.* **31**, 061301 (2014).
- [25] E. Richter-Was, *Phys. Lett. B* **303**, 163 (1993).
- [26] R. M. Baltrusaitis *et al.* (MARK III Collaboration), *Phys. Rev. Lett.* **56**, 2140 (1986). *Phys. Rev. Lett.* **60**, 89 (1988);
- [27] M. Ablikim *et al.* (BESIII Collaboration), *Phys. Rev. Lett.* **122**, 071802 (2019).
- [28] M. Ablikim *et al.* (BESIII Collaboration), *Phys. Rev. Lett.* **122**, 121801 (2019).
- [29] M. Ablikim *et al.* (BESIII Collaboration), *Phys. Rev. D* **99**, 072002 (2019).
- [30] D. Becirevic and A. B. Kaidalov, *Phys. Lett. B* **478**, 417 (2000).
- [31] T. Becher and R. J. Hill, *Phys. Lett. B* **633**, 61 (2006).
- [32] M. Ablikim *et al.* (BESIII Collaboration), *Phys. Rev. D* **108**, 092003 (2023).
- [33] M. Ablikim *et al.* (BESIII Collaboration), *Phys. Rev. D* **92**, 112008 (2015).
- [34] M. Ablikim *et al.* (BESIII Collaboration), *Phys. Rev. D* **83**, 112005 (2011).